IOP Conference Series: Materials Science and Engineering

PAPER • **OPEN ACCESS**

A KPCA-based parameterization model for composite materials representation

To cite this article: M Y Xiao *et al* 2019 *IOP Conf. Ser.: Mater. Sci. Eng.* **504** 012109

View the article online for updates and enhancements.

This content was downloaded from IP address 108.61.201.231 on 14/10/2019 at 02:55

IOP Conf. Series: Materials Science and Engineering **504** (2019) 012109 doi:10.1088/1757-899X/504/1/012109

A KPCA-based parameterization model for composite materials representation

M Y Xiao[1], S B Tian[1], Z W Guo[1] and L Xia [2]

[1]Department of Applied Mathematics, Northwestern Polytechnical University, Xi'an 710072, P.R. China.
[2]State Key Laboratory of Digital Manufacturing Equipment and Technology, Huazhong University of Science and Technology, Wuhan, 430074, China.

Corresponding author and e-mail: M Y Xiao, manyuxiao@nwpu.edu.cn.

Abstract. It is supposed that there exist means to generate material microstructure representations by varying processing parameters numerically [1] or experimentally [2], the goal of this work is to establish a parameterized geometrical description model from learning the set of given snapshot instances. In this work, we propose a parameterization model for the representation of the Representative Volume Elements (RVE) of composite materials based on Kernel Principal Component Analysis (KPCA) method. The set of synthetic RVE snapshots governed by a series of control parameters is firstly mapped into a high-dimensional feature space. Then, Principal Component Analysis (PCA) is performed, together with the establishment of approximated response surfaces of the retained PCA projection coefficients. We showcase the performance of KPCA-based surrogate by applying it for an optimal design of the effective mechanical properties of a two-phase composite material.

1. Introduction

The development of both material science and numerical simulation methods enables researchers to control the material microstructure composition to an unprecedented extent [3]. Consequently, it comes naturally to have the desire of developing materials with optimized properties by architecting their microstructures. For data-driven material design, the generation of material microstructure images is an essential procedure that attracts researchers' interests. However, the access to microstructure images is either economically expensive by experiments or time-consuming by numerical simulation [4]. Therefore, there exists a demand for the development of economical and efficient approaches for material image representations.

Xia and Breitkopf [1] recently exploited its application in multiscale structural topology optimization with an approximate constitutive model based on the POD for local material microstructure design. As an extension of Principal Component Analysis (PCA), the Kernel-based Principal Component Analysis (KPCA) [5] has been proved to be more efficient in many fields particularly when dealing with realistic nonlinear problems.

Concerning the representation of material microstructures, Xia et al. [6] proposed a two-level reduced surrogate using PCA and Moving Least Squares (MLS) method. To extend the applicability of the material representation model, KPCA is adopted in the present work for the representation of nonlinearly parameterized material microstructures. The main idea is to map firstly low dimensional linearly non-separable data into a high-dimensional feature space where PCA is performed afterward in

Content from this work may be used under the terms of the Creative Commons Attribution 3.0 licence. Any further distribution of this work must maintain attribution to the author(s) and the title of the work, journal citation and DOI.
Published under licence by IOP Publishing Ltd

the high-dimensional space. After obtaining the reduced low-dimensional feature data from material microstructure image samples, the parametric characterization of the material microstructure is constructed by using the MLS method. Compared with the POD-based model in [6], the KPCA-based parameterization material microstructure model in this paper ensures higher precision. We also apply the model for microstructure optimal design.

The remainder of this paper is organized as follows: Section 2 reminds the basis of KPCA and proposes a KPCA-based microstructure reconstruction method. Section 3 presents the MLS-based parameterization. Section 4 briefly reviews the numerical homogenization approach for periodic composite materials. In Section 5, we showcase the representation model by considering a set of two-phase composite material snapshots and apply it for an optimal design of composite effective mechanical properties. Finally, conclusion and perspectives are given.

2. Kernel principal component analysis

Given a set of centered observations $\boldsymbol{x}^i \in R^N, i = 1,\ldots,M$, and $\sum_{i=1}^{M} \boldsymbol{x}^i = 0$, the main idea of KPCA is to map firstly the original data sets into a high-dimensional feature space $\mathcal{F}$, at which the conventional PCA is performed afterward. The feature space $\mathcal{F}$ is related to the input space R^N by a nonlinear map Φ:

$$\begin{aligned} &\Phi : R^N \to \mathcal{F} \\ &\mathrm{x} \to \Phi(\boldsymbol{x}). \end{aligned} \tag{1}$$

The dimensionality of $\Phi(\boldsymbol{x})$ in feature space $\mathcal{F}$ could be much larger than $\boldsymbol{x}$ in original input space, even infinite [5]. In order to perform PCA, the data has to be centered in $\mathcal{F}$

$$\sum_{i=1}^{M} \tilde{\Phi}(\boldsymbol{x}^i) = 0, i = 1,\ldots,M \tag{2}$$

in which

$$\tilde{\Phi}(\boldsymbol{x}^i) := \Phi(\boldsymbol{x}^i) - \frac{1}{M}\sum_{l=1}^{M} \Phi(\boldsymbol{x}^l). \tag{3}$$

The projection of image $\Phi(\boldsymbol{x})$ onto the principal components is expressed briefly in terms of the kernel function

$$\alpha_k = \sum_{i=1}^{M} \frac{\beta_k^i}{\sqrt{\lambda_k M}} \tilde{k}(\boldsymbol{x}^i, \boldsymbol{x}), \tag{4}$$

in which $\tilde{k}(\boldsymbol{x}^i, \boldsymbol{x}) = k(\boldsymbol{x}^i, \boldsymbol{x}) - \frac{1}{M}\sum_{l=1}^{M} k(\boldsymbol{x}^l, \boldsymbol{x})$.

As in conventional PCA, we retain $m (m \le p \text{ and } m \ll M)$ most energetic principal components.

2.1. Kernel function

In order to compute dot products of the form $\tilde{\Phi}(\boldsymbol{x}^k) \cdot \tilde{\Phi}(\boldsymbol{x}^l)$, kernel function is used to representation of the dot products in $\mathcal{F}$, which allows the evaluation of the dot product in $\mathcal{F}$ without knowing the map. In this work, Gaussian kernel functions is adopted as follows:

$$k(\boldsymbol{x}, \boldsymbol{y}) = \exp\left(-\frac{\|\boldsymbol{x} - \boldsymbol{y}\|}{2\sigma^2}\right). \tag{5}$$

In which, σ is an adjustable parameter depending on sample data.

The preimage issue in KPCA is dicussed in details in the reference [5].

3. Moving least squares approximation

When the parameter set $\boldsymbol{v}$ which generates the $\boldsymbol{x}$ vector is known a priori, the characteristic information mostly exists in $\alpha_i (i=1,\ldots,m)$. We construct a surrogate model by approximation method: within the design domain, the corresponding $\tilde{\alpha}_i (i=1,\ldots,m)$ can be calculated for any given $\boldsymbol{v}$. In this work, moving least squares (MLS)[7] is used. Fitting function $\tilde{\alpha}_i(\boldsymbol{v})$ can be expressed in the local sub-domain

$$\tilde{\alpha}_i(\boldsymbol{v}) = \sum_{j=1}^{l} a_j(\boldsymbol{v}) p_j(\boldsymbol{v}) = \boldsymbol{p}^{\mathrm{T}}(\boldsymbol{v})\boldsymbol{a}(\boldsymbol{v}) \tag{6}$$

where $\boldsymbol{p}(\boldsymbol{v}) = [p_1(\boldsymbol{v}),\ldots,p_l(\boldsymbol{v})]^{\mathrm{T}}$ are the basis functions, and $\boldsymbol{a}(\boldsymbol{v}) = [a_1(\boldsymbol{v}), \ldots, a_l(\boldsymbol{v})]$ are the vector of coefficients, which are the minimizers of the error function

$$J(\boldsymbol{a}) = \sum_{k=1}^{M} w\left(\left\|\boldsymbol{v}-\boldsymbol{v}^k\right\|\right)\left(\tilde{\alpha}_i(\boldsymbol{v}) - \alpha_i^k\right)^2 \tag{7}$$

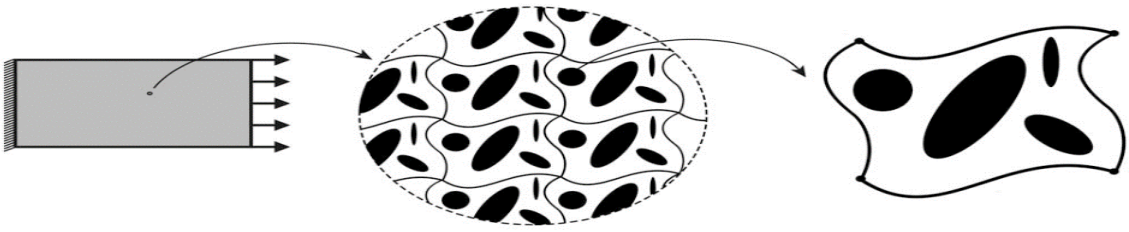
where $w(d)$ are the weights depending on the Euclidean distance d between between $\boldsymbol{v}$ and $\boldsymbol{v}^k$.

4. Numerical homogenization

We assume that the appropriate RVE size has already been selected so as to satisfy the conditions: large enough to be considered in the framework of continuum mechanics and at the same time small enough to be considered surrounded by its own pattern ordered periodically, as illustrated in Figure 1. The homogenization theory uses the periodic boundary conditions (PBC) on the RVE. As stated in [8], the typical PBC is defined as

$$\boldsymbol{u}_b = \bar{\varepsilon} \cdot \boldsymbol{Y}_b + \boldsymbol{u}^* \tag{8}$$

where $\boldsymbol{u}_b$, $\boldsymbol{Y}_b$ are the displacement vector and position vector of considered point on the boundary of the reference configuration, $\bar{\varepsilon}$ is the average strain, $\boldsymbol{u}^*$ is the periodic displacement fluctuation on the boundary surface and it is generally unknown and dependent upon the applied global loads.



(a) Macrostructure (b) Microstructure (c) RVE

Figure 1. Illustration of the selection of a typical 2D representative volume element (RVE) The averaged stress tensor may be obtained [6]

$$\bar{\sigma} = \frac{1}{A}\int_A \sigma(\boldsymbol{y}) dA \tag{9}$$

where A is the current area of the RVE. In the 2D linear elastic case, the constitutive relation of the effective material may be written as following in a matrix notation:

$$\begin{Bmatrix} \bar{\sigma}_{11} \\ \bar{\sigma}_{22} \\ \bar{\sigma}_{12} \end{Bmatrix} = \begin{bmatrix} D_{1111}^{\hom} & D_{1122}^{\hom} & D_{1112}^{\hom} \\ D_{2211}^{\hom} & D_{2222}^{\hom} & D_{2212}^{\hom} \\ D_{1211}^{\hom} & D_{1222}^{\hom} & D_{1212}^{\hom} \end{bmatrix} \begin{Bmatrix} \bar{\varepsilon}_{11} \\ \bar{\varepsilon}_{22} \\ \bar{\gamma}_{12} \end{Bmatrix} \tag{10}$$

where the shear strain $\bar{\gamma}_{12} = 2\bar{\varepsilon}_{12}$. We denote $D^{\hom}$ as the effective elastic stiffness matrix, i.e.

$$\mathbf{D}^{\hom} = \begin{bmatrix} D_{1111}^{\hom} & D_{1122}^{\hom} & D_{1112}^{\hom} \\ D_{2211}^{\hom} & D_{2222}^{\hom} & D_{2212}^{\hom} \\ D_{1211}^{\hom} & D_{1222}^{\hom} & D_{1212}^{\hom} \end{bmatrix} \tag{11}$$

In the paper, finite element analysis method combining PBC is used to calculate the $\mathbf{D}^{\hom}$. Every pixel of material microstructural RVE snapshot is regard as a finite element, whose precision depends on the resolution. In finite element analysis, one node of the mesh of the RVE has to be fixed in order to avoid rigid body motion.

5. Numerical test case

In this paper, on the basis of a set of microstructure RVE sample images which controlling variables are known a priori, we want to reduce the sample data using KPCA method to obtain the feature information of each observation sample. Then, the parametric model of material microstructure representation is constructed using MLS on the coefficients of feature information. With this parameterization representation model, the microstructure RVE image for a given parameter set can be obtained. Therefore, the parameterization representation model can be applied to design an optimal microstructure of the material.

5.1. Image numerical representation

Given a material microstructural snapshot which pixel is $N \times N$, as shown in Figure 2. The white and black colors correspond to two distinct material phases. Suppose the image matrix is $\mathrm{Im}_{N\times N}$, the corresponding binary matrix $[\mathbf{S}]_{N\times N}$ is given straightforwardly as:

$$[\mathbf{S}]_{ij} = \begin{cases} 1 & \text{if } [Im]_{ij} \text{ is material A} \\ 0 & \text{if } [Im]_{ij} \text{ is material B.} \end{cases} \tag{12}$$

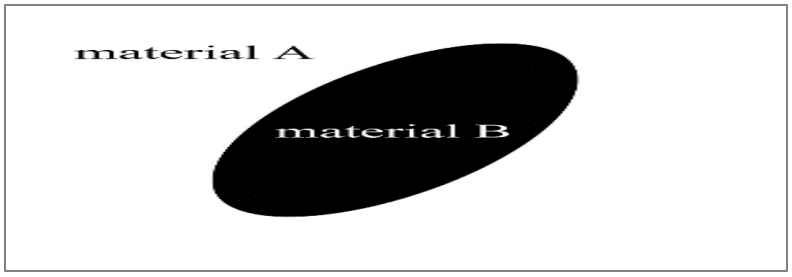


Figure 2. Snapshot representation of a two-phase material microstructure.

In order to perform KPCA reduction, each matrix $\mathbf{S}^k$ is restored in a vector $\boldsymbol{x}^k$ of length N^2 attributed with real values instead of binary values.

5.2. Construction of microstructure image sample

In this section, we consider a commonly investigated periodic two-phase microstructure pattern containing 4 elliptical inclusions as shown in Figure 3(a). The geometric parameters of the elliptical inclusions are given in Figure 3(b). Microstructure of this form could be used for the modeling of various

material types. Suppose the total area of the inclusion phase is 30% of the total area of the RVE. By linking the parameters of the inclusions to two randomly generated controlling variables $\boldsymbol{v} = [v_1; v_2](v_1, v_2 \in [0,1])$, 441 binary snapshots of resolution 128×128 are generated with a uniform sampling of v_1 and v_2. As given by the parameterization function in Table 1, the radius and the rotations of the ellipse inclusions are associated with v_1 and v_2, respectively. In this paper quadratic basis $\boldsymbol{p}(\boldsymbol{v}) = [1, v_1, v_2, {v_1}^2, v_1 v_2, {v_2}^2]^{\mathrm{T}}$ and a Gaussian weightin -g function $w(d)$ are chosen:

$$w(d) = e^{-d^2/h^2}, \tag{13}$$

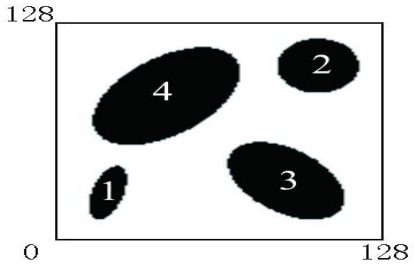
where d is the Euclidean distance between $\boldsymbol{v}$ and $\boldsymbol{v}_k$, h is a spacing parameter that may be used to smooth out small features in the data. Here we choose h=0.03.

5.3. KPCA reconstruction errors

When a series of material microstructure RVE images are generated upon the above setting, the reconstruction errors w.r.t. the number of retained modes can be written as:

$$\delta(m) = \frac{\sum_{k=1}^{M} (\boldsymbol{x}_k - \tilde{\boldsymbol{x}}_k)^{\mathrm{T}} (\boldsymbol{x}_k - \tilde{\boldsymbol{x}}_k)}{\sum_{j=1}^{M} \boldsymbol{x}_j^{\mathrm{T}} \boldsymbol{x}_j} \tag{14}$$

where $\tilde{\boldsymbol{x}}_k$ is the reconstructed image vector, $\boldsymbol{x}_k$ is the corresponding raw image vector. The curves of reconstruction error of KPCA versus PCA is shown in Figure 4.



(a). Original snapshot

	area ratio	R_0	θ_0	x_0	y_o
1	2%	6	15°	100	20
2	5%	16.1	0°	25	102
3	9%	16	135°	93	90
4	14%	20	45°	43	43

(b). The parameters of the inclusions

Figure 3. Original snapshot and the parameters of the inclusions.

Table 1.Parameterization function of v w.r.t. R, r and θ of the inclusions.

	R	r	θ
Elliptical inclusion 1	$(1+v_1^2)R_0$	$\frac{2\%S}{\pi R}$	$\theta_0 + 90v_2^{1/2}$
Elliptical inclusion 2	R_0	$\frac{5\%S}{\pi R}$	0
Elliptical inclusion 3	$(1+v_1^2)R_0$	$\frac{9\%S}{\pi R}$	$\theta_0 + 90v_2^{1/2}$
Elliptical inclusion 4	$(1+0.5v_1^2)R_0$	$\frac{14\%S}{\pi R}$	$\theta_0 + 90v_2^{1/2}$

From Figure 4 we can observe that compared to PCA method, KPCA method requires retaining many less numbers of modes for same number reconstruction error. For instance, using 10 KPCA

modes, the reconstruction errors are 4%, whilst with 10 modes for PCA, the reconstruction errors are up to 6%.

5.4. Test case about optimal design of material effective mechanical properties

The material properties of glass fiber/epoxy resin composite in the reference [9] is used. The Young's modulus $E_m = 3.5Gpa$, Poisson ratio $\nu_m = 0.35$. The Young's modulus of glass fiber reinforcement $E_i = 70Gpa$, Poisson ratio $\nu_i = 0.35$. The volume fraction of the glass fiber component is 45%. The young's modulus of intermediate values can be obtained through interpolation approximation

$$E = \frac{x}{255} \times E_i + (1 - \frac{x}{255}) \times E_m \tag{15}$$

where x is the gray value of corresponding point in microstructure images of material.

As the effective elastic properties of the material can be evaluated by homogenization, the homogenized properties of the composite can be improved by optimizing the control parameters.

Based on the microstructure model, we optimize the bulk modulus K^{hom} and the shear G^{hom} modulus of corresponding material given by

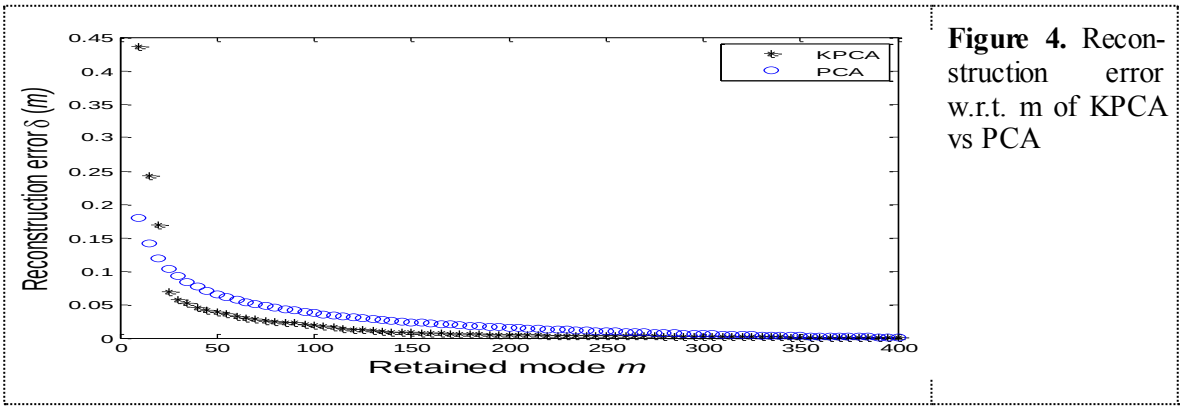
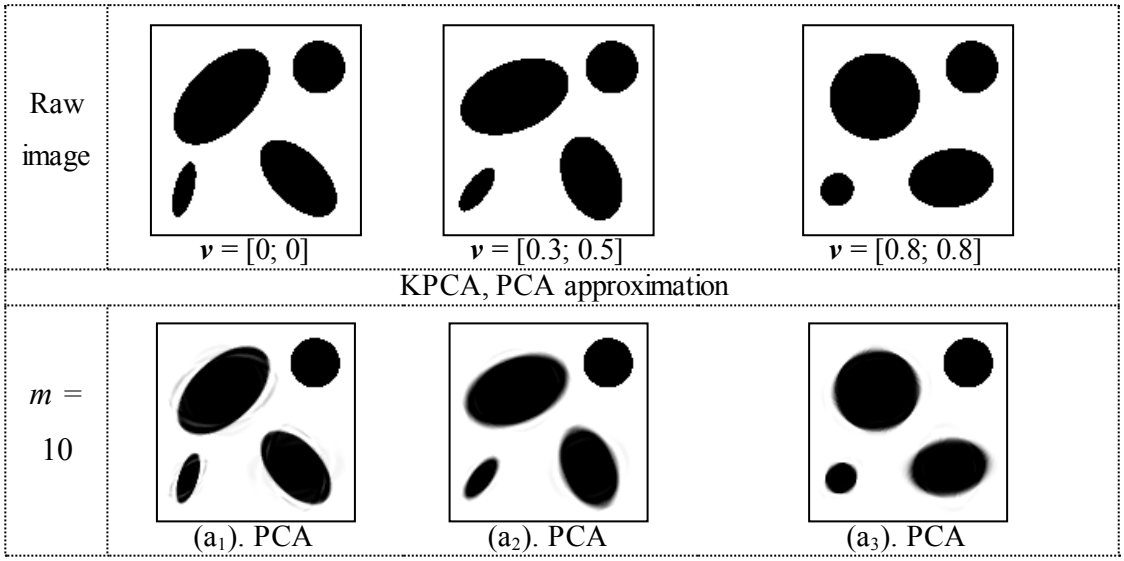


Figure 4. Reconstruction error w.r.t. m of KPCA vs PCA



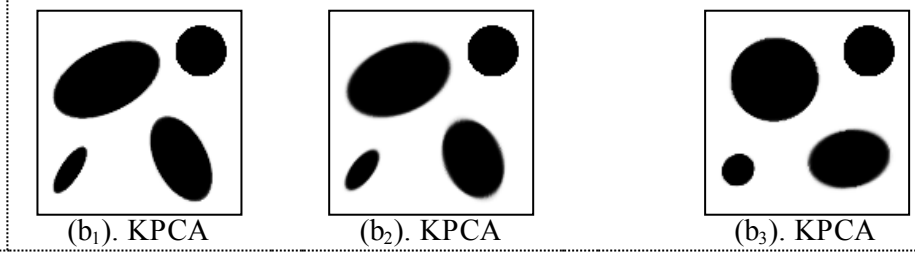


Figure 5. The reconstruction results of different *m*.

$$\begin{aligned} K^{\text{hom}} &= \left(D_{1111}^{\text{hom}} + D_{1122}^{\text{hom}} + D_{2211}^{\text{hom}} + D_{2222}^{\text{hom}}\right)/4 \\ G^{\text{hom}} &= D_{1212}^{\text{hom}} \end{aligned} \tag{16}$$

By solving two optimization problems with boundary constraints respectively, the optimal parameter values $\boldsymbol{v}_1^*, \boldsymbol{v}_2^*$, corresponding to the maximum $\tilde{K}^{\text{hom}}(\boldsymbol{v})$ and $\tilde{G}^{\text{hom}}(\boldsymbol{v})$ can be obtained:

$$\begin{aligned} \boldsymbol{v}_1^* &= \text{Argmax}\left(\tilde{K}^{\text{hom}}(\boldsymbol{v}), \boldsymbol{v} \in \Omega, \Omega = [0,1]\times[0,1]\right); \\ \boldsymbol{v}_2^* &= \text{Argmax}\left(\tilde{G}^{\text{hom}}(\boldsymbol{v}), \boldsymbol{v} \in \Omega, \Omega = [0,1]\times[0,1]\right). \end{aligned} \tag{17}$$

The optimization problem can be solved by genetic algorithm [10] in Matlab, the initial population size is 20, selection strategy is stochastic uniform, and adaptive feasible function is used to control mutation. According to the 0-1 cross, randomly generating genetic binary vectors. The optimization results are as follows

$$K(\boldsymbol{v}_1^*) = \max\left(\tilde{K}(\boldsymbol{v})\right) = 6.5922, \text{when } \boldsymbol{v}_1^* = [0.195, 0.949]^{\text{T}},\ G(\boldsymbol{v}_2^*) = \max\left(\tilde{G}(\boldsymbol{v})\right) = 2.2338, \text{when } \boldsymbol{v}_2^* = [0.219, 0.128]^{\text{T}}. \tag{18}$$

6. Conclusions

This paper has proposed a parameterization surrogate model for material microstructure representation using KPCA and MLS approximation. It has been shown that the established KPCA-based surrogate enables an efficient and effective representation of the RVE in the nonlinear context compared to conventional PCA-based surrogates. The KPCA-based surrogate has also been applied for the design of the effective mechanical properties of a two-phase composite material with respect to the controlling parameters.

Acknowledgement

This work has been supported by the National Natural Science Foundation of China (11302173) and the Natural Science Foundation of Shaanxi Province (2017JQ1037).

References

[1] Liang X, Raghavan B, Breitkopf P 2017 Towards surrogate modeling of material microstructures through the processing variables, Applied Mathematics & Computation 294 157–168
[2] Tian T, Cheng L, Xing J, et al 2017 Effects of sintering on the microstructure and electrical properties of zno-based thermoelectric materials, Materials & Design 132 479–485
[3] Torquato S 2010 Optimal design of heterogeneous materials, Annual Review of Materials Research 40 101–129
[4] Engler O, Hirsch J 2002 Texture control by thermomechanical processing of aa6xxx almgsi sheet alloys for automotive applicationsa review, Materials Science and Engineering A336 (1–2) 249–262
[5] Scholkopf B, Mika S, Burges C J C, Knirsch P, Muller K, Ratsch G, Smola A J 1999 Input

space versus feature space in kernel-based methods, IEEE TRANSACTIONS ON NEURAL NETWORKS 1000–1017
[6] Xia L, Breitkopf P 2014 A reduced multiscale model for nonlinear structural topology optimization, Computer Methods in Applied Mechanics and Engineering 280 (280) 117–134
[7] Lancaster P, Salkauskas K 1981 Surfaces generated by moving least squares methods, Mathematics of Computation 37 (155) 141–158
[8] Suquet P 1987 Elements of homogenization theory for inelastic solid mechanics, in: A. zaoui, e. sanchez-palencia (eds.), Homogenization Techniques for Composite Media 194–275
[9] Lukkassen D, Wall P 1995 Some engineering and mathematical aspects on the homogenization method, Composites Engineering 5 (5) 519–531
[10] Zhao J 2011 Optimization technology and matlab optimization toolbox, China Machine Press 173–181